POLYNOMIAL EXPANSION OF THE STAR FORMATION HISTORY IN GALAXIES

D. Jiménez-López, P. Corcho-Caballero, S. Zamora, Y. Ascasibar

Universidad Autónoma de Madrid

FACULTAD DE CIENCIAS
UNIVERSIDAD AUTÓNOMA DE MADRID

A&A, Forthcoming article, https://doi.org/10.1051/0004-6361/202141338

INDEX

THE POLYNOMIAL METHOD

THE POLYNOMIAL METHOD

Reconstruction
of the SFH

THE POLYNOMIAL METHOD

Reconstruction of the SFH

- Non-paremetric methods
- Parametric methods

THE POLYNOMIAL METHOD

Reconstruction of the SFH

Non-paremetric methods

- + High accuracy
- + Flexible
- - Excesive computational time
- - Degenerancies

prospector

$$\Psi(t) \sim \sum_{i=0}^{\infty} c_i \delta_i$$

Parametric methods

THE POLYNOMIAL METHOD

Reconstruction of the SFH

Non-paremetric methods

- \+ High accuracy
- \+ Flexible
- \- Excesive computational time
- \- Degenerancies

$$\Psi(t) \sim \sum_{i=0}^{\infty} c_i \delta_i$$

PROSPECTOR

Parametric methods

- \+ Few parameters
- \- Limited due to simplicity

$$\Psi(t)\ \alpha\ e^{-t/\tau}$$

$$\Psi(t)\ \alpha\ e^{-\frac{(t'-t)}{2\sigma^2}}$$

$$\Psi(t)\ \alpha\ \frac{t}{\tau} e^{-t/\tau}$$

CIGALE

THE POLYNOMIAL METHOD

Reconstruction of the SFH

Non-paremetric methods

- + High accuracy
- + Flexible
- - Excesive computational time
- - Degenerancies

$$\Psi(t) \sim \sum_{i=0}^{\infty} c_i \delta_i$$

Parametric methods

- + Few parameters
- - Limited due to simplicity

$$\Psi(t)\ \alpha\ e^{-t/\tau}$$

$$\Psi(t)\ \alpha\ e^{-\frac{(t'-t)}{2\sigma^2}}$$

$$\Psi(t)\ \alpha\ \frac{t}{\tau}\, e^{-t/\tau}$$

Polynomial method

Flexibility + Velocity

THE POLYNOMIAL METHOD

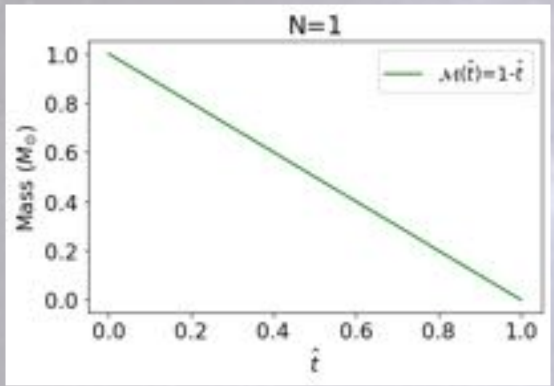

Figure 1. Primordial polynomial MFH asociated to each N-degree basis.

THE POLYNOMIAL METHOD

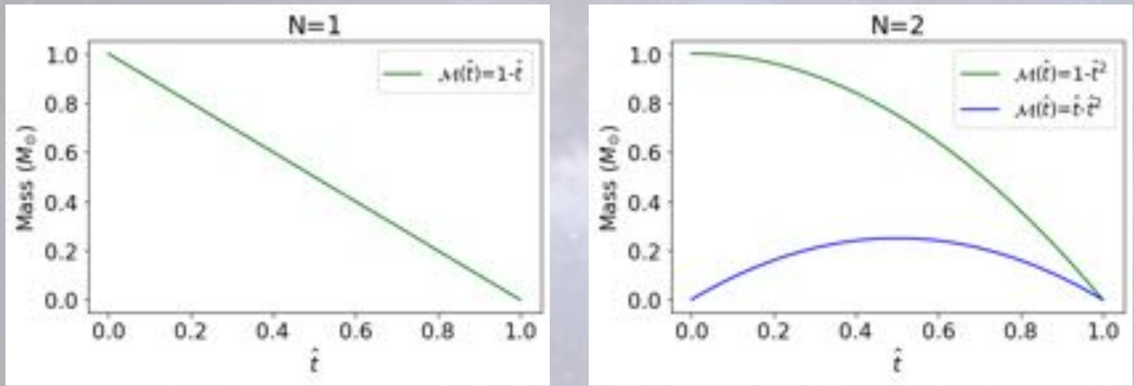

Figure 1. Primordial polynomial MFH asociated to each N-degree basis.

THE POLYNOMIAL METHOD

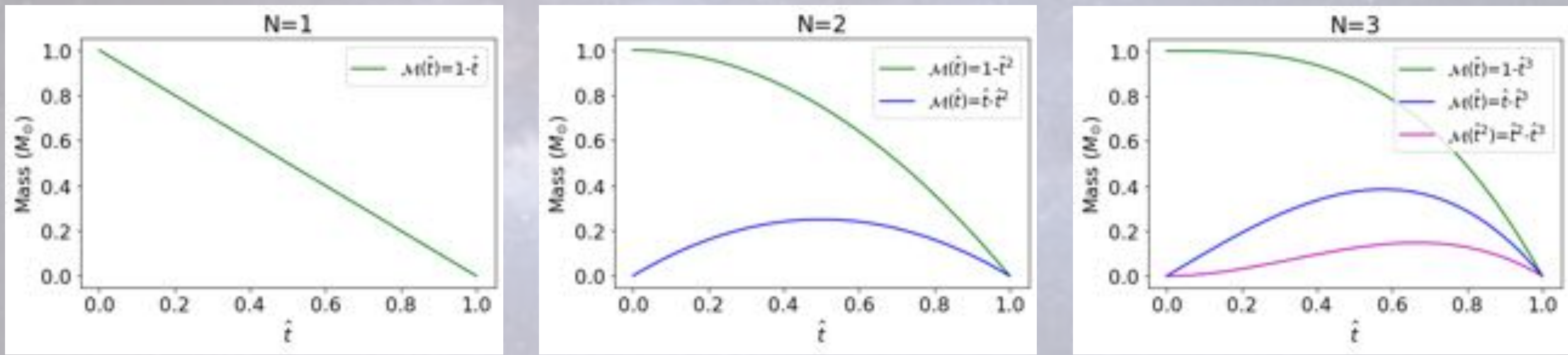

Figure 1. Primordial polynomial MFH asociated to each N-degree basis.

THE POLYNOMIAL METHOD

N_ν = 3 observables

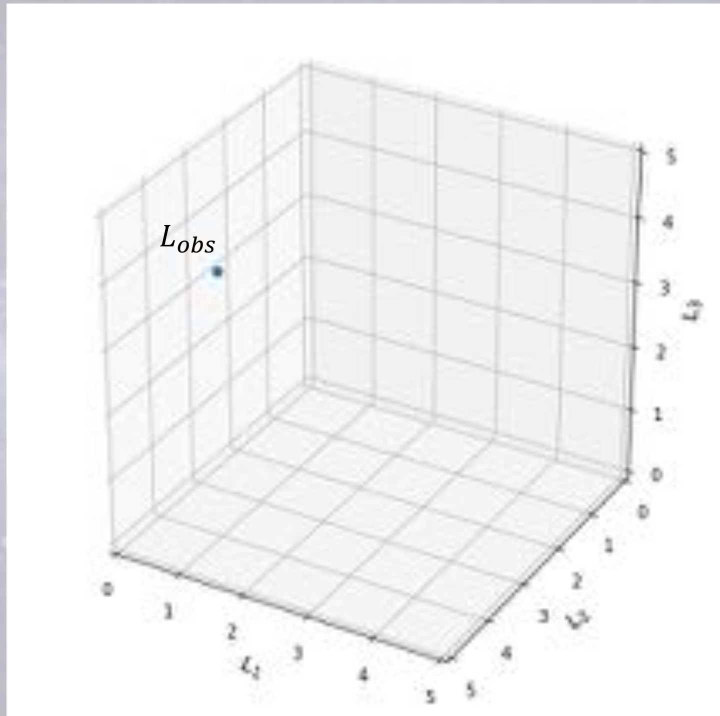

Figure 2. Luminosity coverage on the N_ν = 3 case

THE POLYNOMIAL METHOD

$$N = N_\nu$$

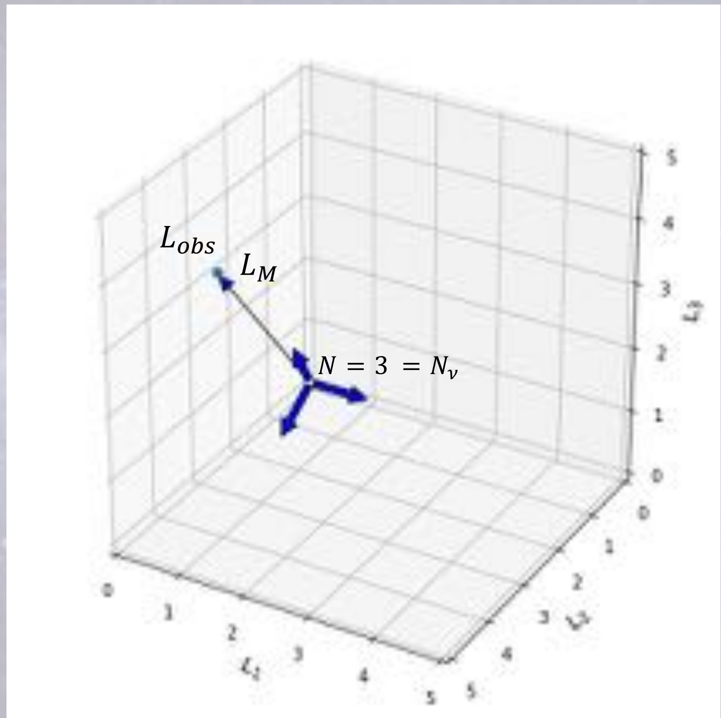

Figure 2. Luminosity coverage on the N_ν = 3 case

THE POLYNOMIAL METHOD

$N < N_\nu$

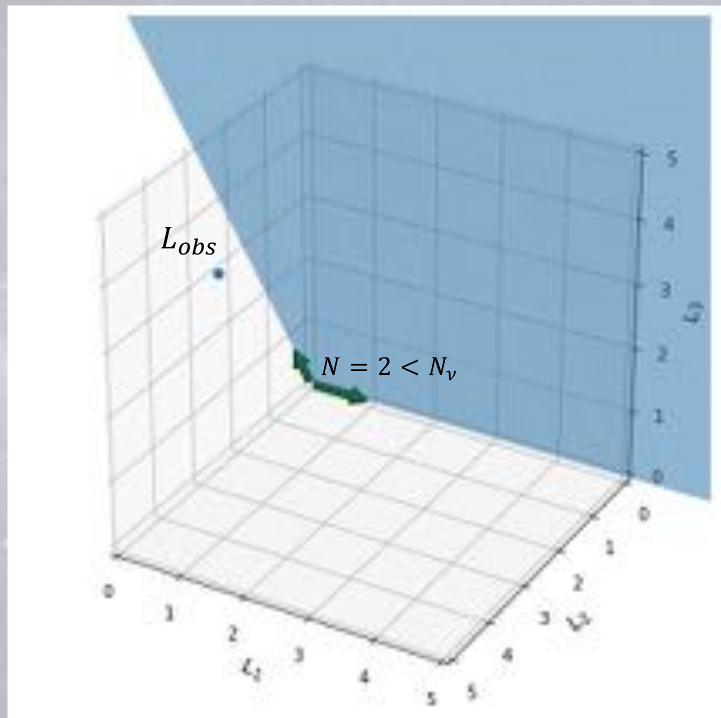

Figure 2. Luminosity coverage on the N_ν = 3 case

THE POLYNOMIAL METHOD

N_ν = 3 observables

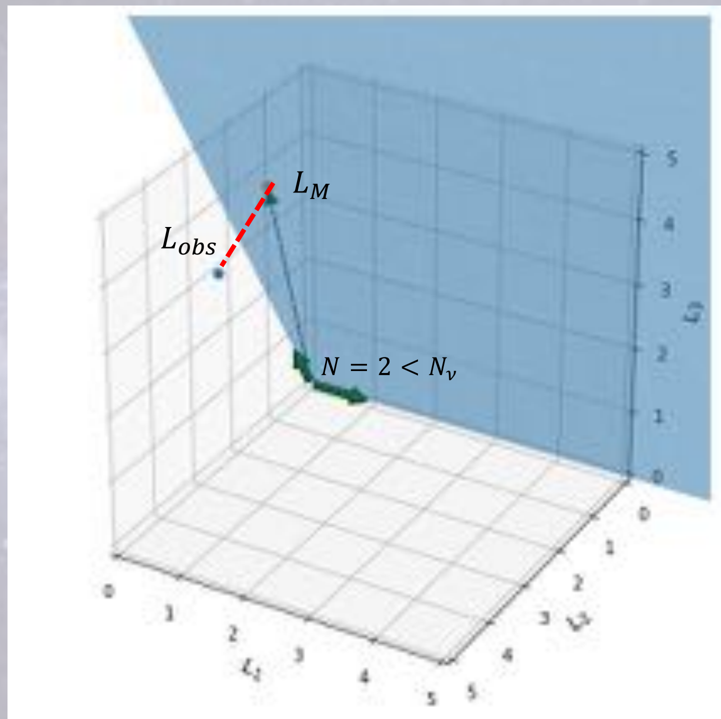

Figure 2. Luminosity coverage on the N_ν = 3 case

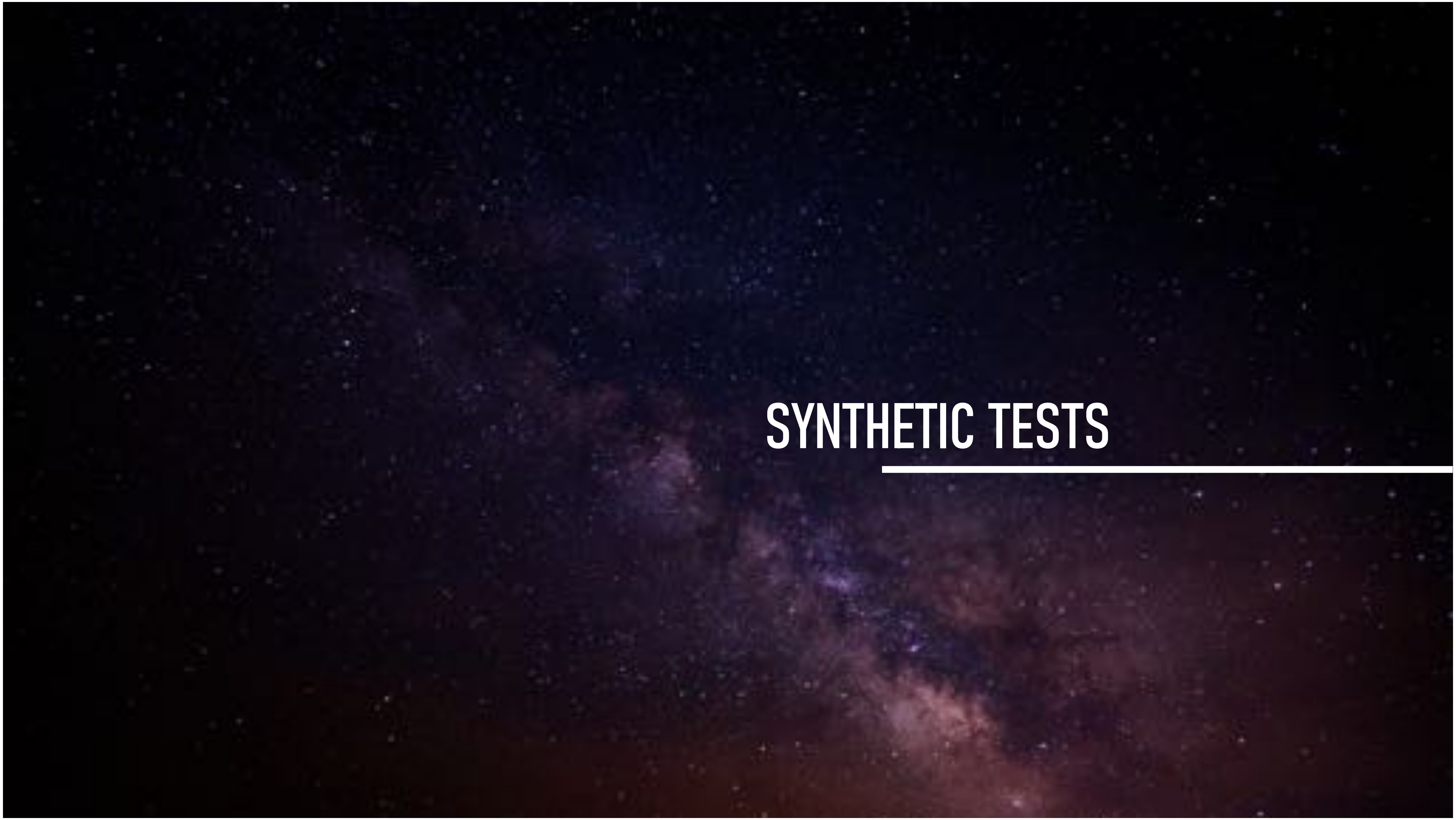
SYNTHETIC TESTS

SYNTHETIC TESTS

Synthetic
SFH

SYNTHETIC TESTS

Input parameters

τ, FWHM, α

Synthetic SFH

SYNTHETIC TESTS

Input parameters

τ, FWHM, α

Synthetic SFH

“Observed” luminosities

L_{obs}

SYNTHETIC TESTS

Input parameters

τ, FWHM, α

Synthetic SFH

"Observed" luminosities

L_{obs}

Best fit coefficients

SYNTHETIC TESTS

Input parameters

τ, FWHM, α

Synthetic SFH

"Observed" luminosities

L_{obs}

Best fit coefficients

Polynomial reconstruction

SYNTHETIC TESTS

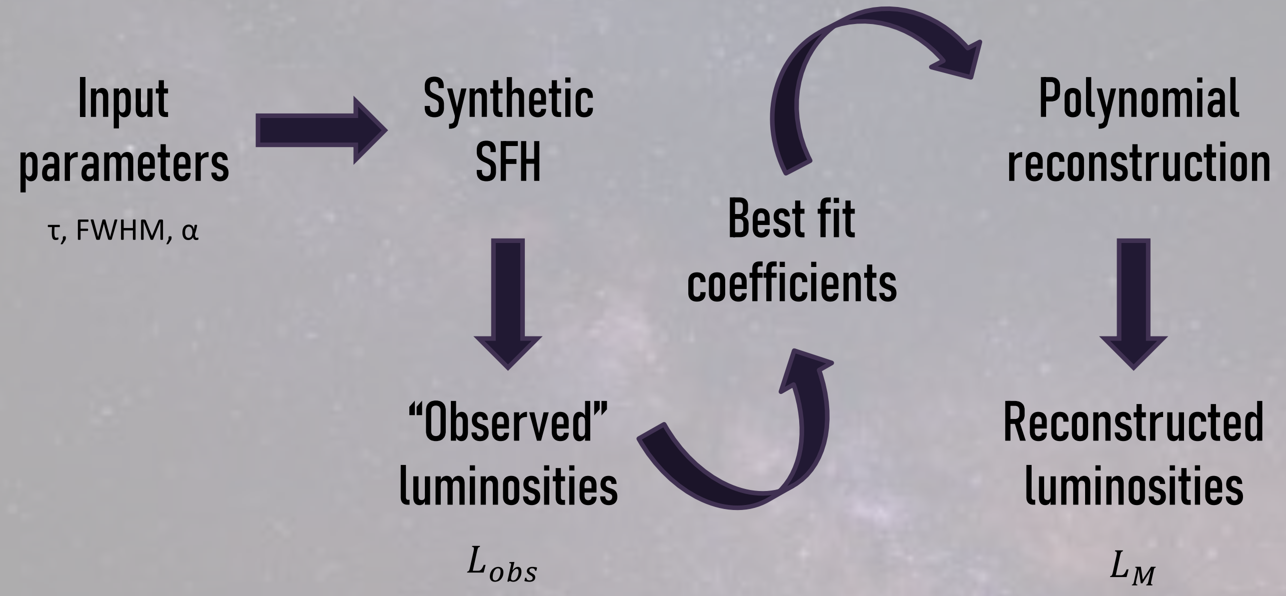

SYNTHETIC TESTS

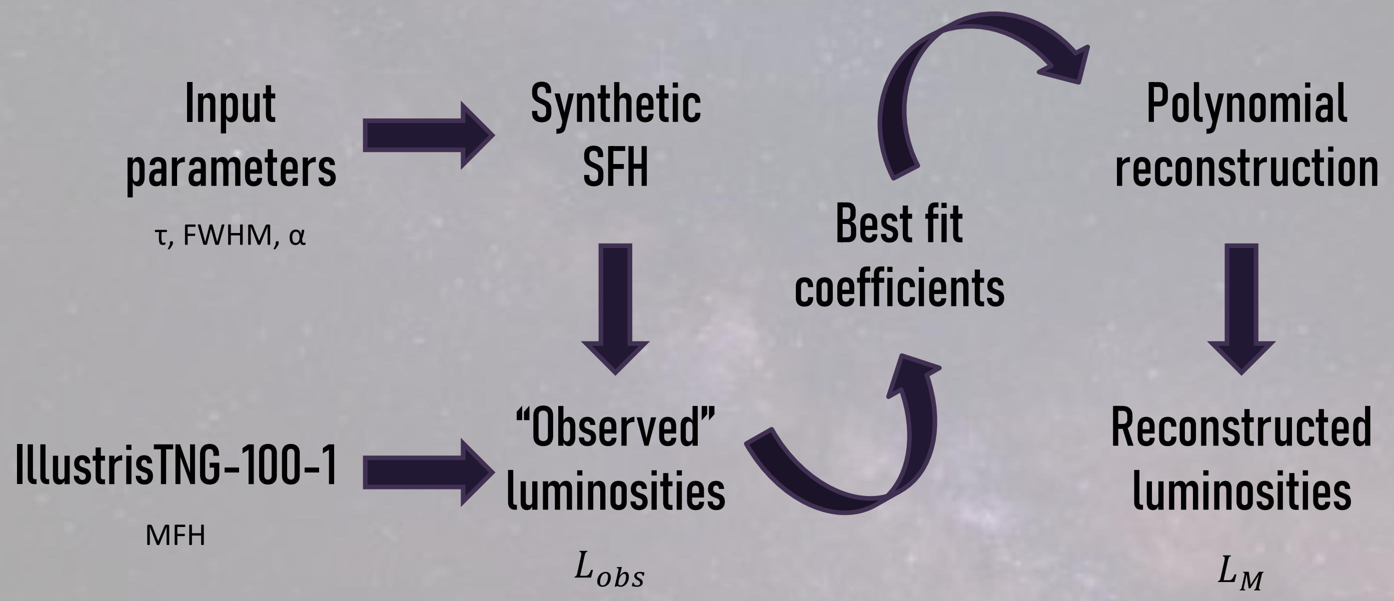

FIT QUALITY

FIT QUALITY

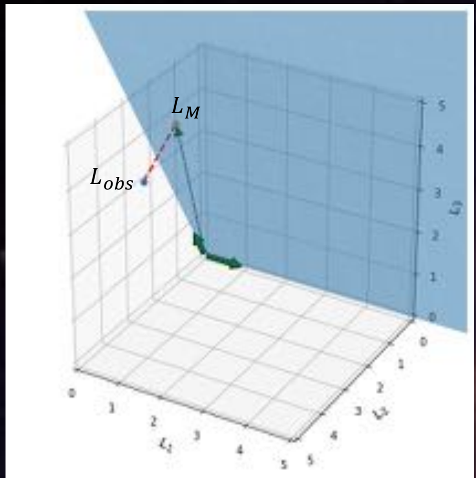

$$\Psi(t) \propto e^{-t/\tau}$$

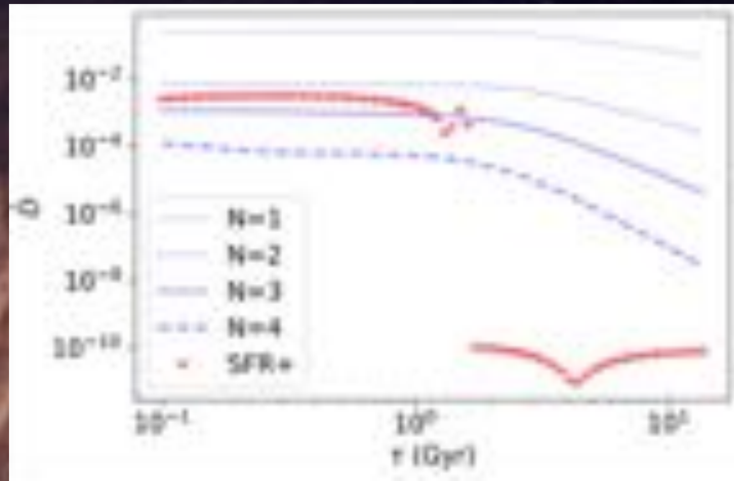

$$\Psi(t) \propto \frac{t}{\tau} e^{-t/\tau}$$

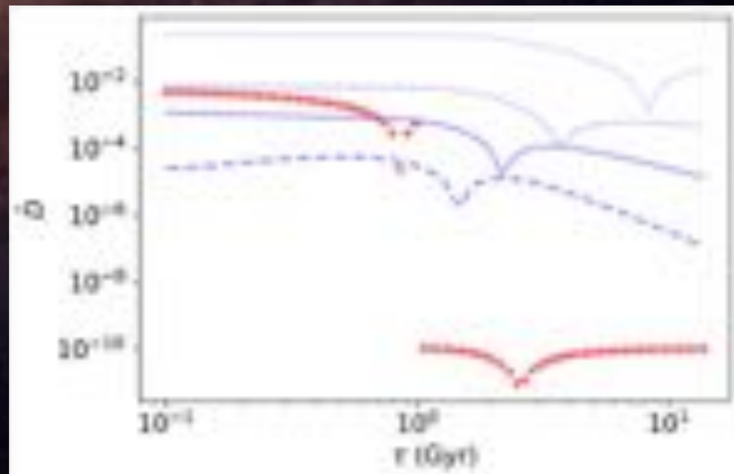

Figure 3. Best fitting normalized distances associated with each polynomial degree, N (blue lines) and the best positive-SFR fit (red crosses) for different characteristic times of the exponential (upper panel) and delayed-τ (bottom panel) analytical models.

FIT QUALITY

$$\Psi(t) \propto e^{\frac{-(t_0-\alpha-t)^2}{2\sigma^2}}$$

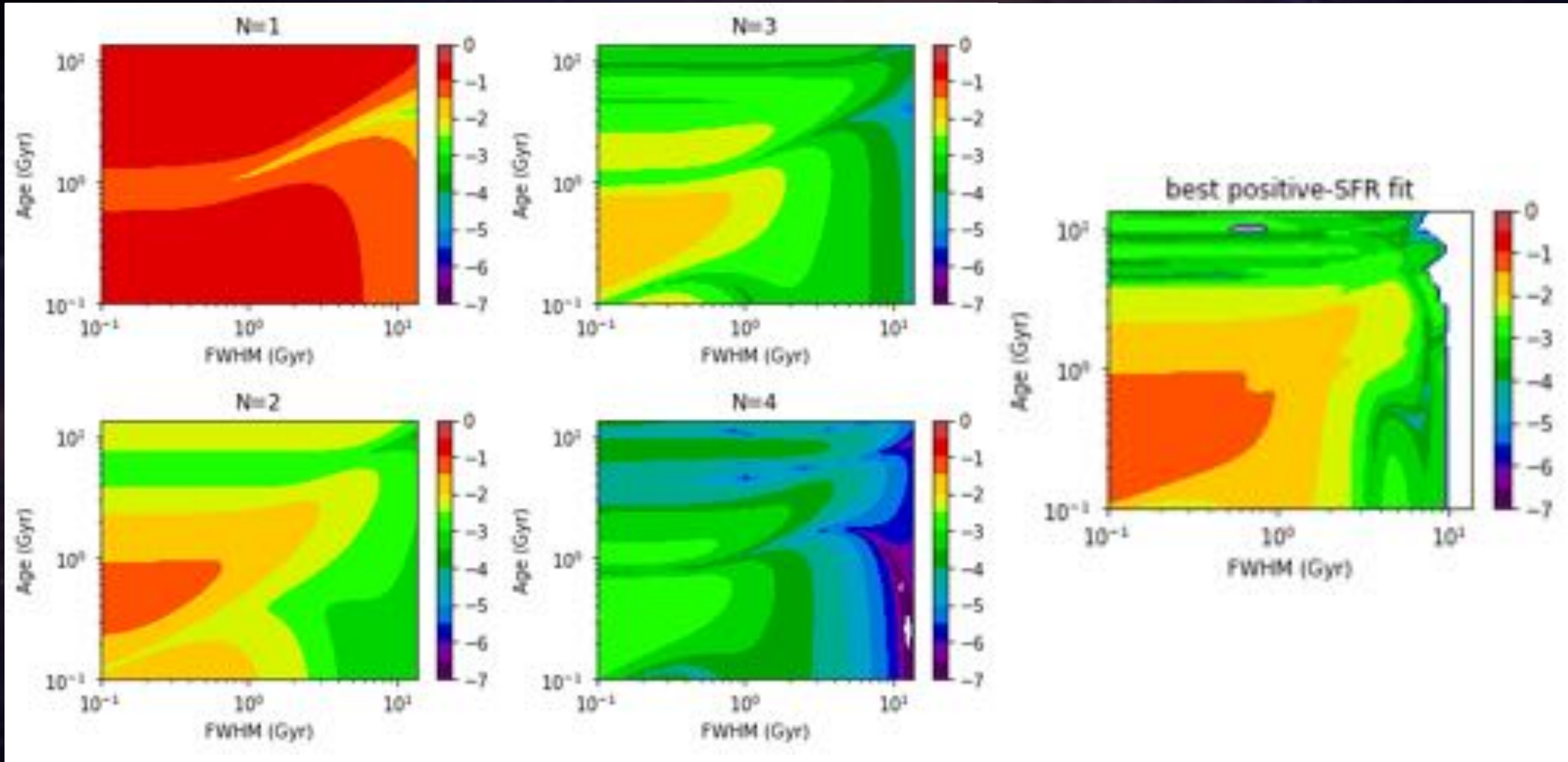

Figure 4. Best fitting normalized distances associated with each polynomial degree, N, and the best positive-SFR fit for different ages and FWHMs of the Gaussian synthetic SFHs.

FIT QUALITY

IllustrisTNG-100-1

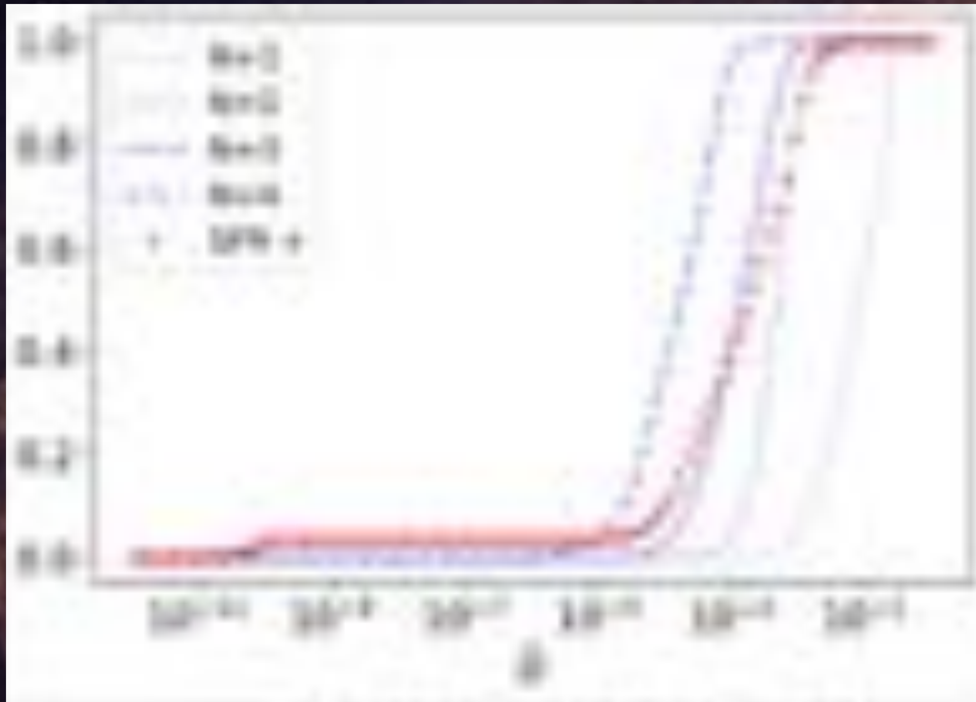

Figure 5. Fraction of galaxies of the Illustris sample with distances under a certain value, for each polynomial degree, N (blue lines) and the best positive-SFR fit (red crosses).


QUALITY OF THE RECONSTRUCTION

QUALITY OF THE RECONSTRUCTION

$$\Psi(t)\ \alpha\ e^{-t/\tau}$$

$$\Psi(t)\ \alpha\ \frac{t}{\tau} e^{-t/\tau}$$

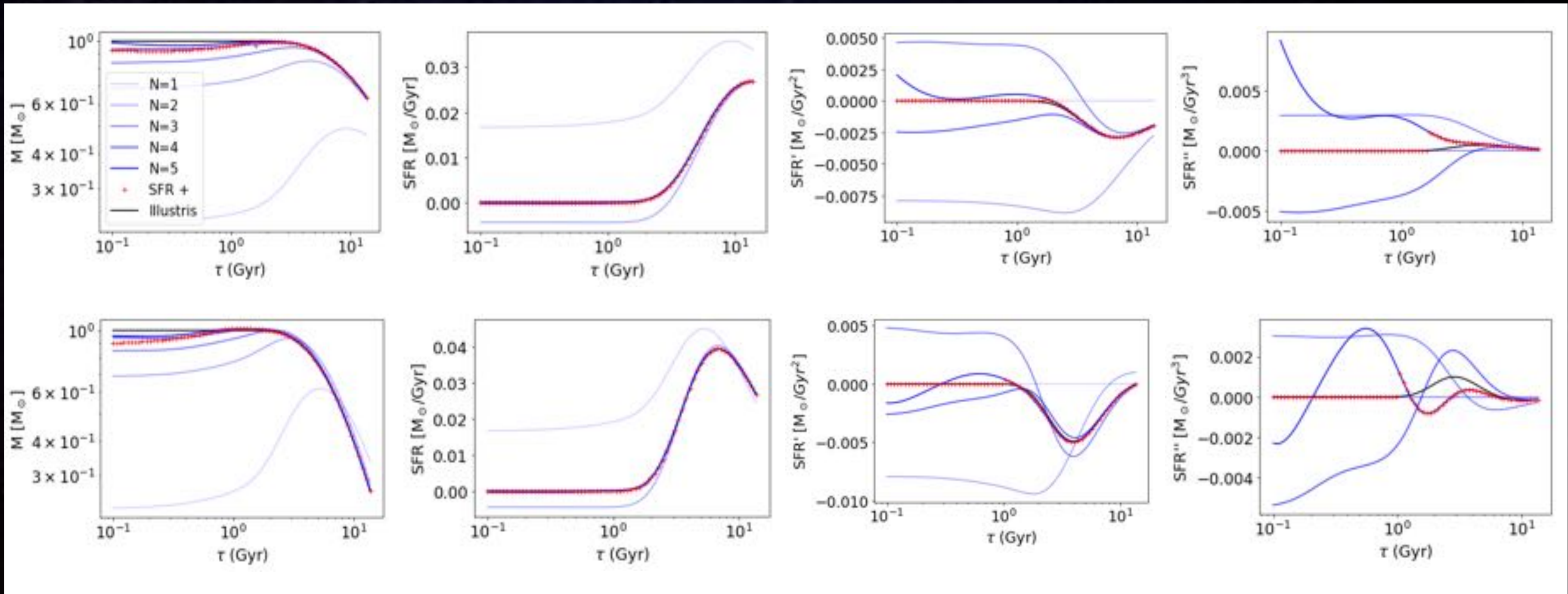

Figure 6. Estimates of the MFH reconstructed at the present time for the exponential (upper row) and delayed-τ (bottom row) synthetic SFHs with different timescales, τ, compared with the correct values (solid black lines). Red crosses correspond to the best positive-SFR fit.

QUALITY OF THE RECONSTRUCTION

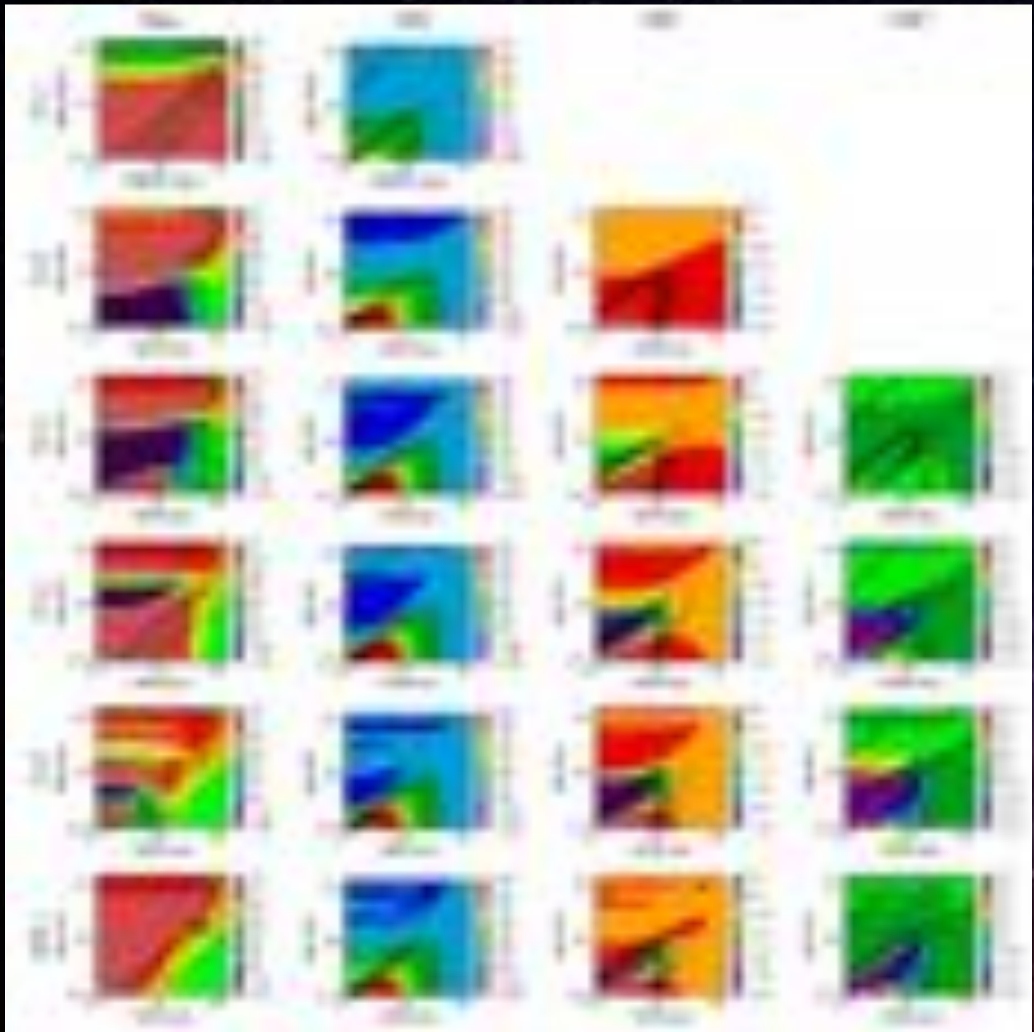

$$\Psi(t)\ \alpha\ e^{\frac{-(t_0-\alpha-t)^2}{2\sigma^2}}$$

Figure 7. Estimates of the MFH reconstructed at the present time for the Gaussian synthetic SFHs with different ages and FWHMs, compared with the correct values (black contours).

QUALITY OF THE RECONSTRUCTION

IllustrisTNG-100-1

$$\delta M(\hat{t}) = \frac{\Delta M_{poly} - \Delta M_{sim}}{|\Delta M_{poly}| + |\Delta M_{sim}|}$$

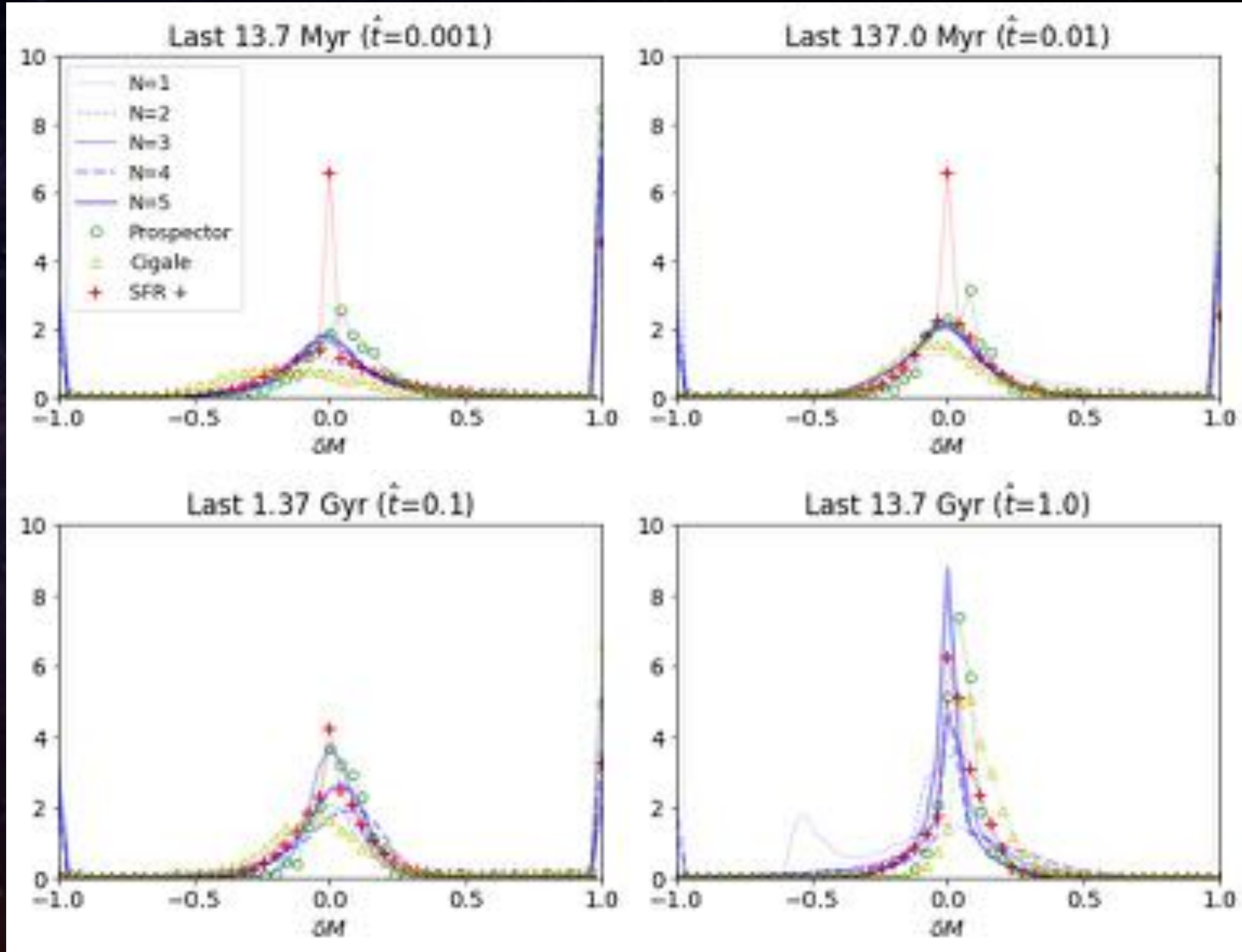

Figure 8. Probability densities of the δM, for different values of the normalized lookback time for the polynomial methods (blue lines), the best positive-SFR fit (red crosses), the Prospector model (green circles), and the Cigale fit (yellow triangles).


RECONSTRUCTED HISTORIES

EXPONENTIAL SFH

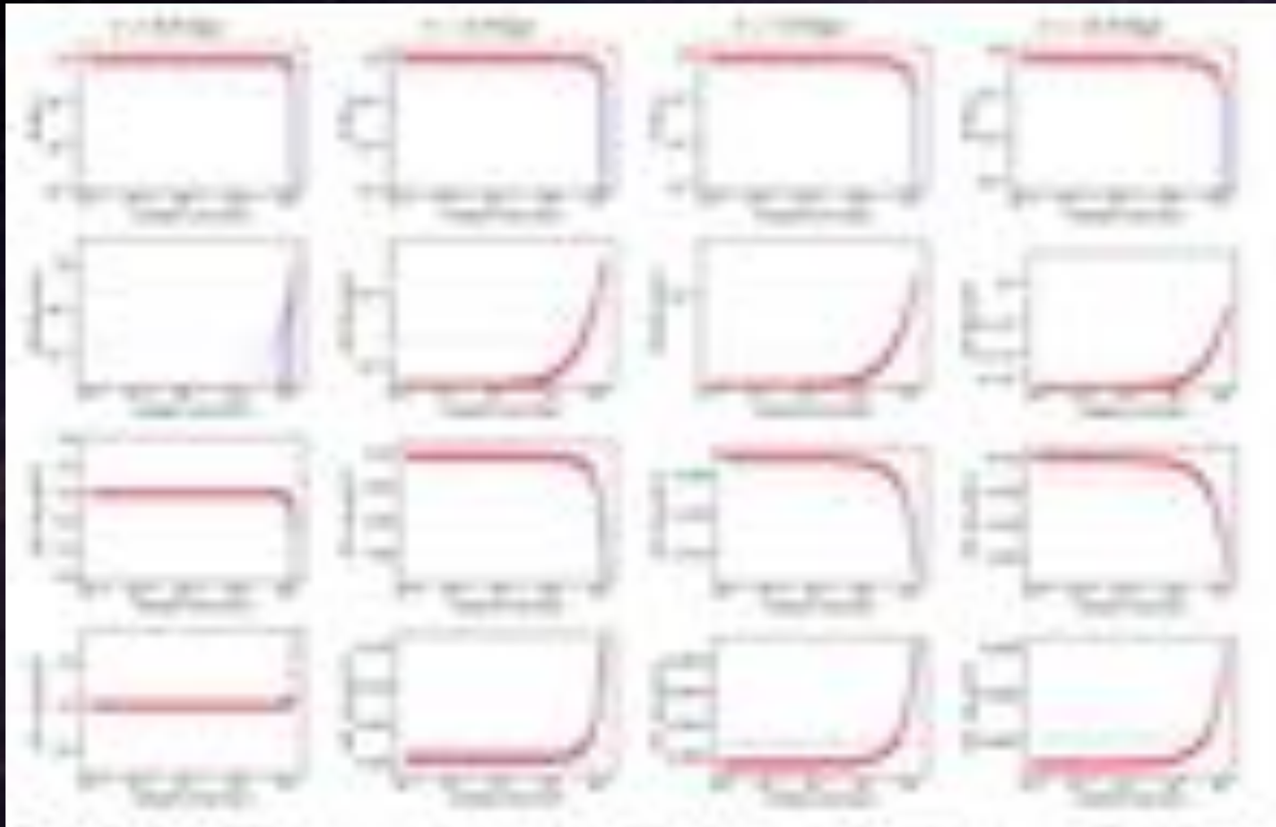

Figure 9. MFHs reconstructed from a sample of synthetic exponential SFR with different timescales τ, with our parametric model (blue lines) and the best positive-SFR fit (red crosses) compared to the input model (solid black line).

DELAYED -τ SFH

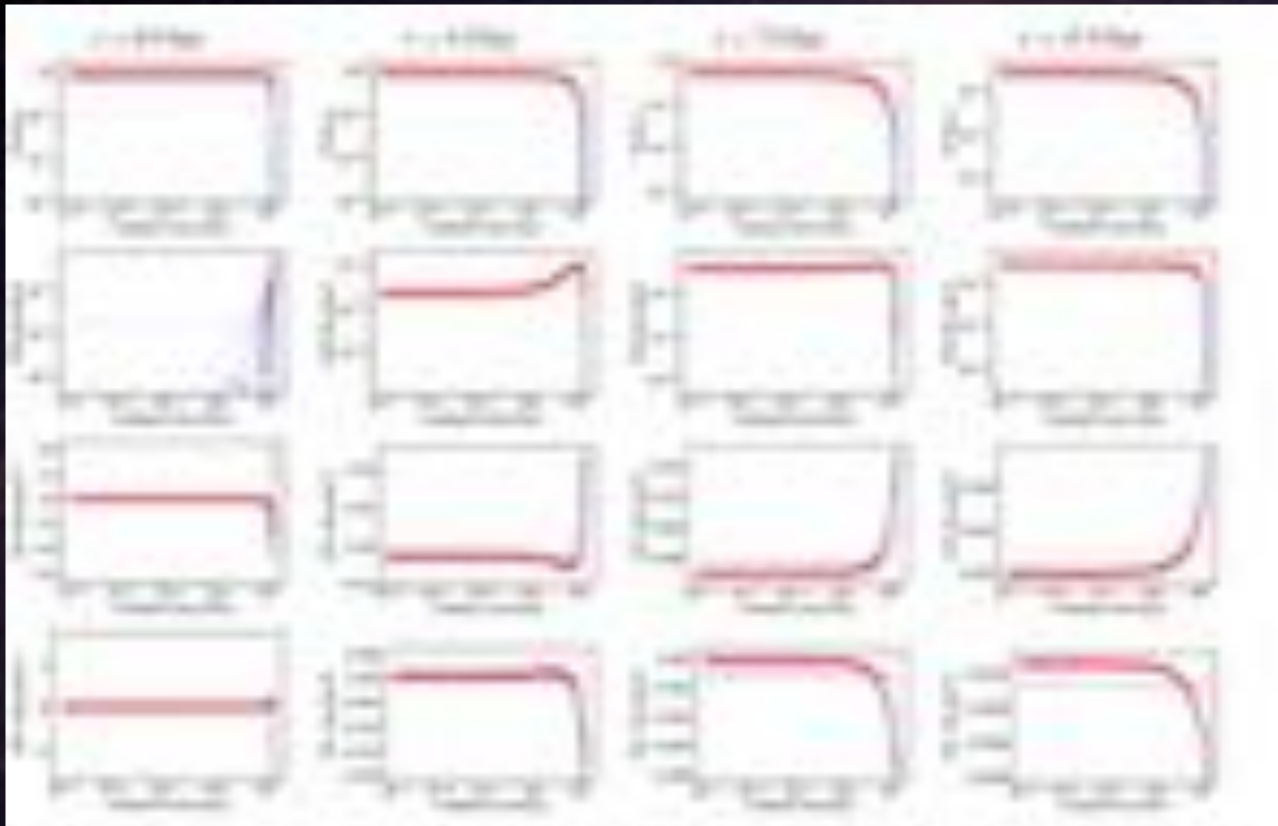

Figure 10. MFHs reconstructed from a sample of synthetic exponential-delayed SFR with different timescales τ, with our parametric model (blue lines) and the best positive-SFR fit (red crosses) compared to the input model (solid black line).

GAUSSIAN SFH: M($\hat{t}$)

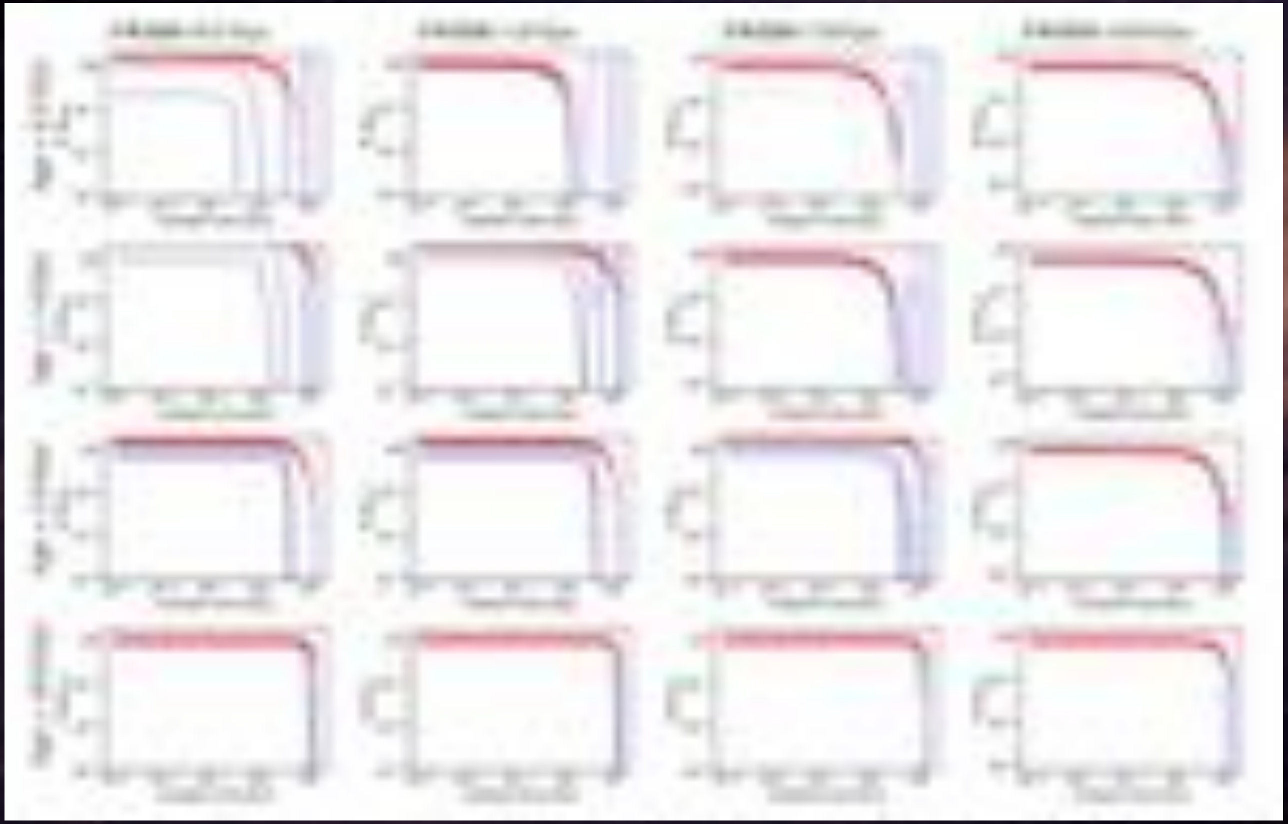

Figure 11. Mass formation history reconstructed for a sample of synthetic Gaussian SFR with different peak age and FWHM, with our parametric model (blue lines) and the best positive-SFR fit (red crosses) compared to the input model (solid black line).

GAUSSIAN SFH: $\Psi(\hat{t})$

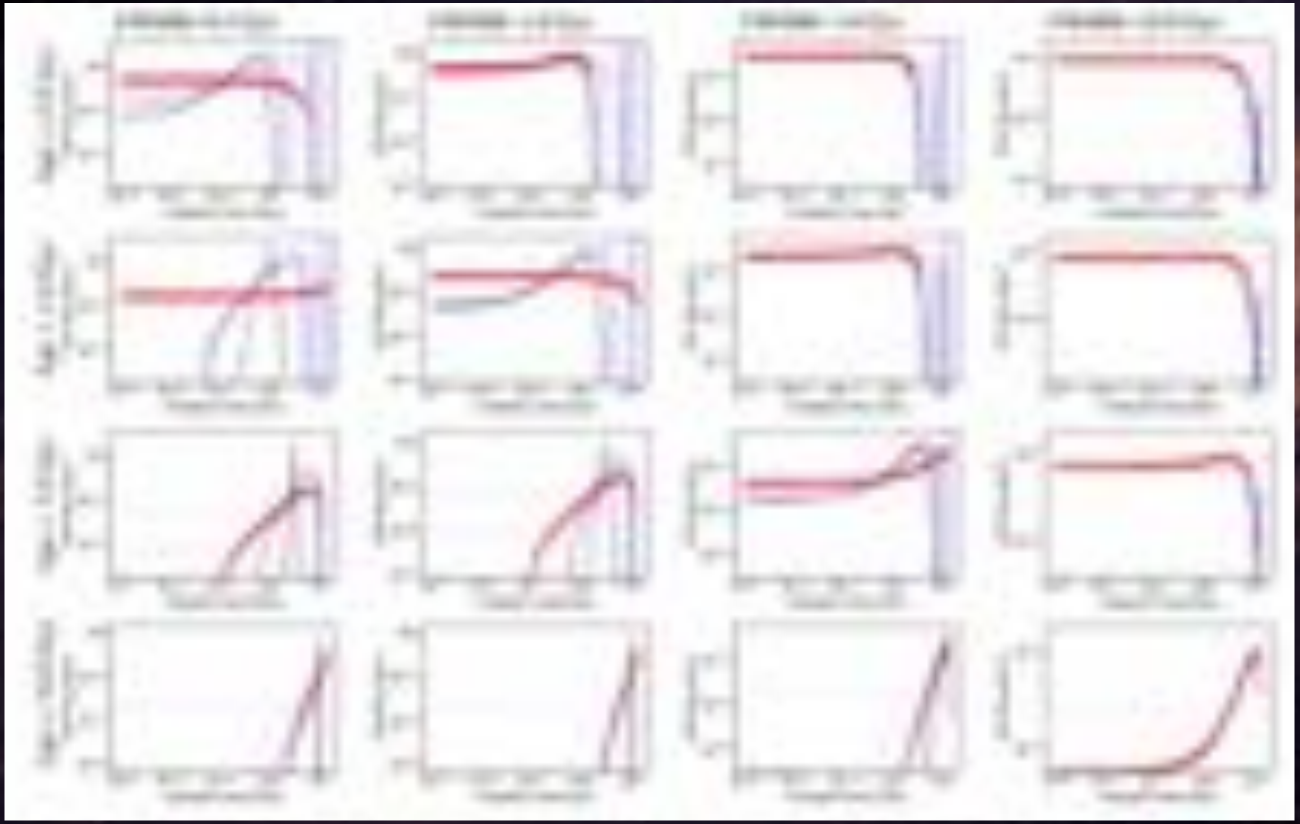

Figure 12. Star formation rate reconstructed for a sample of synthetic Gaussian SFR with different peak age and FWHM, with our parametric model (blue lines) and the best positive-SFR fit (red crosses) compared to the input model (solid black line).

GAUSSIAN SFH: $\dot{\Psi}(\hat{t})$

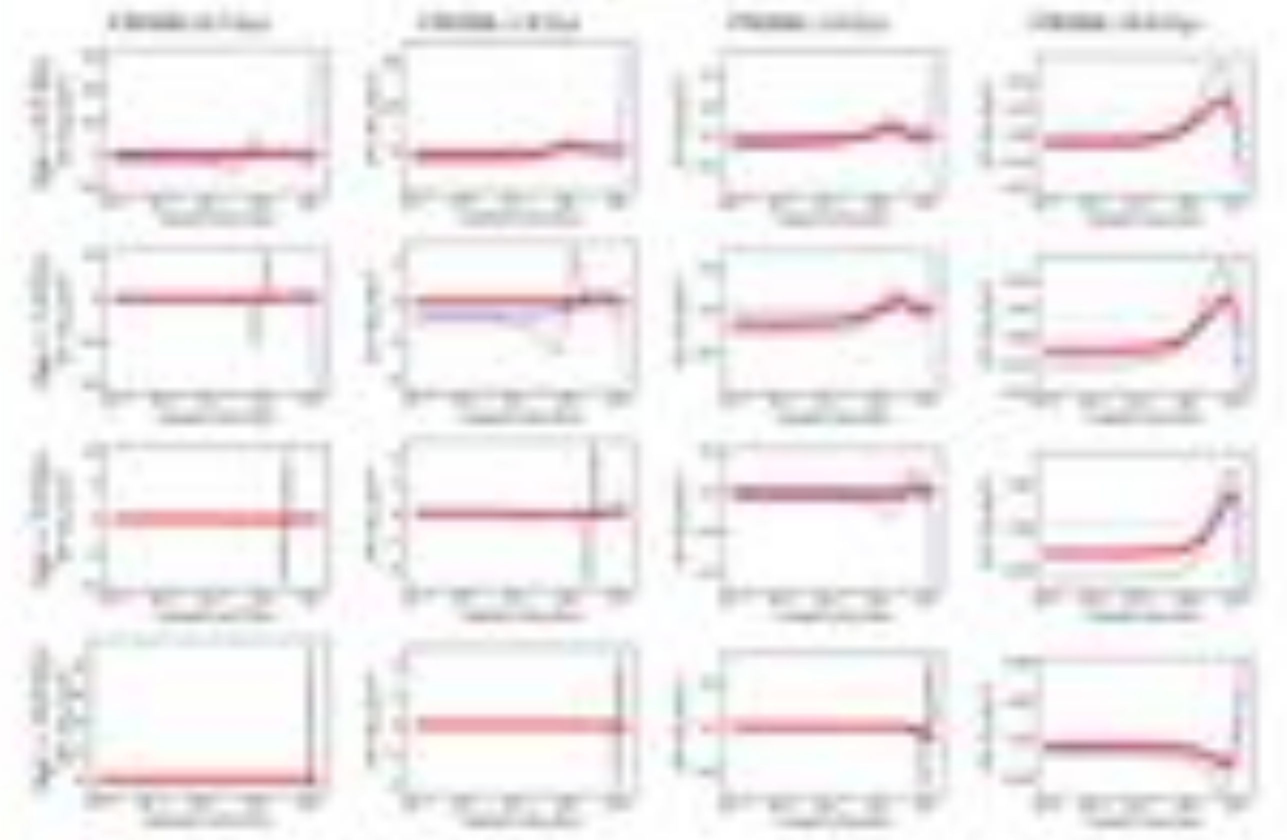

Figure 13. Time derivative of the star formation rate reconstructed for a sample of synthetic Gaussian SFR with different peak age and FWHM, with our parametric model (blue lines) and the best positive-SFR fit (red crosses) compared to the input model (solid black line).

Illustris sample: M($\hat{t}$)

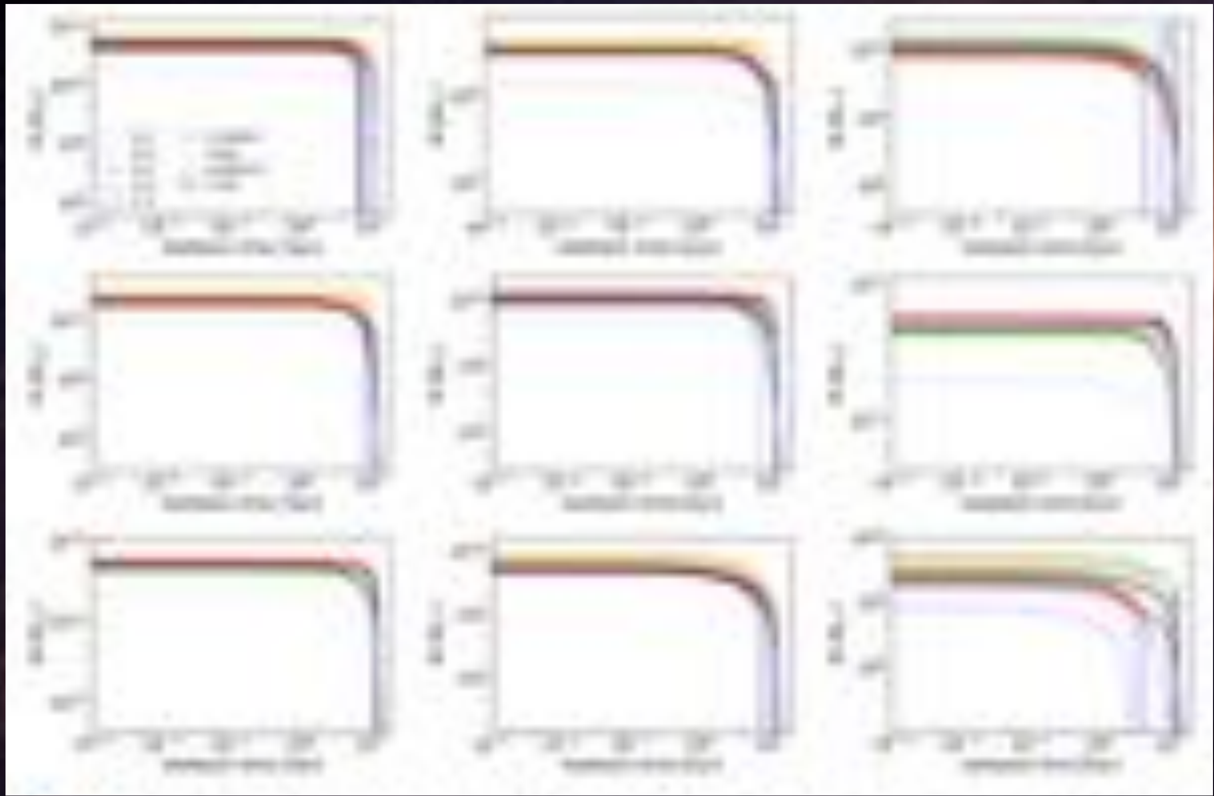

Figure 14. Mass formation history reconstructed for some of the galaxies of the Illustris sample with our polynomial model (blue lines), the best positive-SFR fit (red crosses), Prospector (green circles) and Cigale (yellow triangles), compared to the imput model (black solid lines)

Illustris sample: $\Psi(\hat{t})$

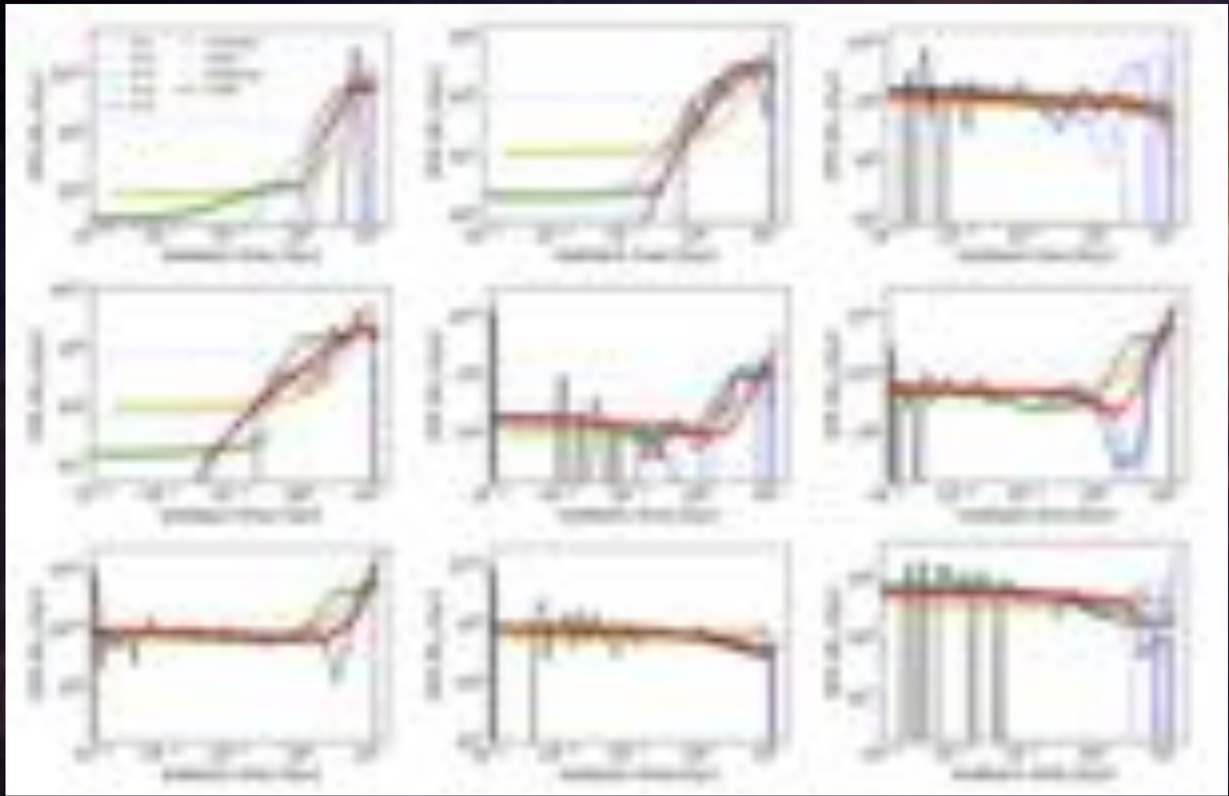

Figure 15. Star formation rate reconstructed for some of the galaxies of the Illustris sample with our polynomial model (blue lines), the best positive-SFR fit (red crosses), Prospector (green circles) and Cigale (yellow triangles), compared to the imput model (black solid lines)


CONCLUSIONS

CONCLUSIONS

- Method improves with:
  - Higher characteristic timescales
  - Higher polynomia degrees

CONCLUSIONS

- Method improves with:
  - Higher characteristic timescales
  - Higher polynomia degrees
- Weakness:
  - Short timescales variations
  - Early peaks

CONCLUSIONS

- Method improves with:
  - Higher characteristic timescales
  - Higher polynomia degrees
- Weakness:
  - Short timescales variations
  - Early peaks
- Strength:
  - High computational velocity (< 1 sec/fit)
  - Simple and accurate

CONCLUSIONS

- Method improves with:
  - Higher characteristic timescales
  - Higher polynomia degrees
- Weakness:
  - Short timescales variations
  - Early peaks
- Strength:
  - High computational velocity (< 1 sec/fit)
  - Simple and accurate
- Ongoing work:
  - Observational errors
  - Bayesian treatment
  - Metallicity
  - Dust extintion
  - t_{in} and t_f as free parameters


THANK YOU FOR
YOUR ATTENTION

SUPPLEMENTARY MATERIAL - OBS. ERRORS & BAYESIAN TREATMENT

$$\hat{M}(t) = 1 - e^{\frac{\hat{t}-1}{0,5}}$$

$$\Delta u = \pm 2\%$$
$$\Delta g, r, i, z = \pm 1\%$$

$$\chi^2 = \sum_{i=ugriz} \frac{(L_{model_i} - L_{obs_i})^2}{(\Delta L_{obs_i})^2}$$

$$\omega_i(t) = \frac{e^{-2,5\cdot\chi^2}}{\sigma(t)_i{}^2}$$

$$\mathrm{B}ay(t) = \frac{\sum_{i=1}^{N} M_i \omega_i}{\sum_{i=1}^{N} \omega_i}$$

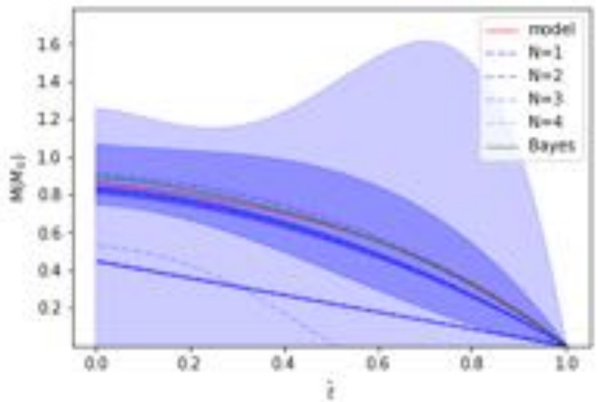

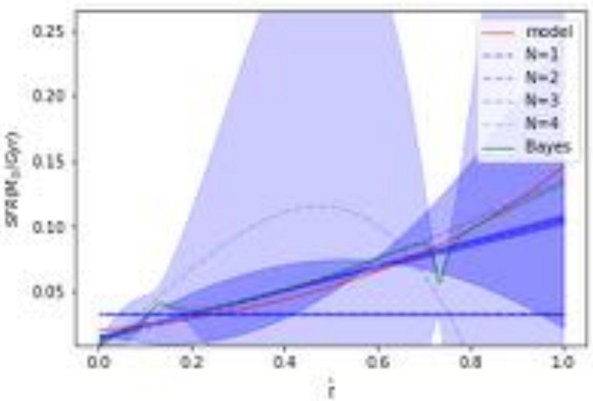

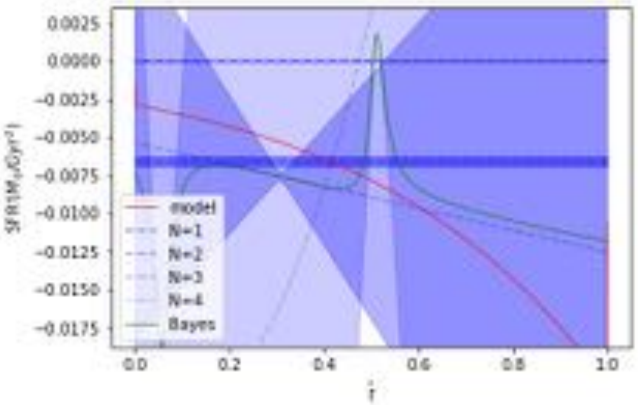

S1. Example of observational errors and bayesian treatments.

SUPPLEMENTARY MATERIAL - MATHEMATICAL FORMALISM

$$M^{(N)}(\hat{t}) = \sum_{i} \delta_i^{(N)} B_i^{(N)}(\hat{t})$$

$$B_i^{(N)}(\hat{t}) = \sum_{n=0}^{i} \beta_{n,i}^{(N)} \mathcal{M}_n^{(N)}(\hat{t}) \qquad \delta_i^{(N)} = \sum L_{\mathrm{obs}}(\nu)\, L_i^{(N)}(\nu)$$

$$\mathcal{M}_n^{(N)}(\hat{t}) = \hat{t}^n - \hat{t}^N \qquad L_i^{(N)}(\nu) = \sum^{i} \beta_{n,i}^{(N)} \mathcal{L}_n^{(N)}(\nu)$$

$$B_i^{(N)}(\hat{t}) \cdot B_j^{(N)}(\hat{t}) = \delta_{ij} \qquad L_M(\nu) = \sum_{i} \delta_i^{(N)} L_i^{(N)}(\nu)$$

$$d^2 = \sum \left[L_M(\nu) - L_{\mathrm{obs}}(\nu)\right]^2$$

$$L(\nu) = \int_0^{t_0} \Psi(t)\, \mathcal{L}_{\mathrm{SSP}}(\nu, t_0 - t)\, \mathrm{d}\hat{t}$$

S2. Compilation of mathematical formulas used in this work.